Angular (Gothic) aortic arch leads to enhanced systolic wave reflection, central aortic stiffness, and increased left ventricular mass late after aortic coarctation repair: Evaluation with magnetic resonance flow mapping

Phalla Ou, MD,[a,b] David S. Celermajer, MBBS, DSc, FRACP,[c] Olivier Raisky, MD,[d] Odile Jolivet, PhD,[a] Fanny Buyens, MS,[a] Alain Herment, PhD,[a] Daniel Sidi, MD, PhD,[e] Damien Bonnet, MD, PhD,[e] and Elie Mousseaux, MD, PhD[a,f]

Objective: We sought to investigate the mechanism whereby a particular deformity of the aortic arch, an angulated Gothic shape, might lead to hypertension late after anatomically successful repair of aortic coarctation.

Methods: Fifty-five normotensive patients with anatomically successful repair of aortic coarctation and either a Gothic (angulated) or a Romanesque (smooth and rounded) arch were studied with magnetic resonance angiography and flow mapping in both the ascending and descending aortas. Systolic waveforms, central aortic stiffness, and pulse velocity were measured. We hypothesized that arch angulation would result in enhanced systolic wave reflection with loss of energy across the aortic arch, as well as increased central aortic stiffness.

Results: Twenty patients were found to have a Gothic, and 35 a Romanesque, arch. Patients with a Gothic arch showed markedly augmented systolic wave reflection (12 ± 6 vs 5 ± 0.3 mL, $P < .001$) and greater loss of systolic wave height in the distal aorta ($30\% \pm 16\%$ vs $22\% \pm 12\%$, $P < .01$) compared with that of subjects with a Romanesque arch. Pulse wave velocity was also increased with a Gothic arch (5.6 ± 1.1 vs 4.1 ± 1 m/s, $P < .0001$), as well as left ventricular mass index (85 ± 15 vs 77 ± 20 g/m^2). Patients with a Romanesque arch had increased aortic stiffness compared with that of control subjects (stiffness β-index, 3.9 ± 0.9 vs 2.9 ± 1; $P = .03$).

Conclusions: Angulated Gothic aortic arch is associated with increased systolic wave reflection, as well as increased central aortic stiffness and left ventricular mass index. These findings explain (at least in part) the association between this pattern of arch geometry and late hypertension at rest and on exercise in subjects after coarctation repair.

From INSERM UMR_S678,[a] CHU la Pitié-Salpétrière, Paris, France; the Departments of Pediatric Radiology,[b] Pediatric Cardiovascular Surgery,[d] and Pediatric Cardiology,[e] UFR Necker-Enfants Malades, University Rene Descartes Paris V, AP-HP, Paris, France; and the Department of Medicine,[c] University of Sydney, Sydney, Australia; and the Department of Cardiovascular Radiology,[f] Hôpital Européen Georges Pompidou, University Rene Descartes Paris V, AP-HP, Paris, France.

Supported by a grant from the Fondation Wyeth pour la Santé de l'Enfant et de l'Adolescent (France) and from the Fédération Française de Cardiologie (France).

Received for publication Sept 28, 2006; revisions received March 14, 2007; accepted for publication March 29, 2007.

Address for reprints: Phalla Ou, MD, Department of Pediatric Radiology, Hôpital Necker-Enfants Malades, 149, rue de Sèvres 75743 Paris Cedex 15, France (E-mail: phalla.ou@nck.ap-hop-paris.fr).

J Thorac Cardiovasc Surg 2008;135:62-8

0022-5223/$34.00

doi:10.1016/j.jtcvs.2007.03.059

Despite early and anatomically successful repair, patients with coarctation of the aorta (CoA) still remain at high risk for cardiovascular events. The major adverse prognostic factor includes late hypertension, which occurs in 20% to 40% of survivors of anatomically successful repair.[1-5]

The pathophysiology of abnormal blood pressure in this setting is still unclear. Different mechanisms have been proposed, including, for example, mild residual stenosis at the coarctectomy site, hyperreactivity of the renin-angiotensin system, impairment of the baroreflex system, impairment of peripheral vascular reactivity, and increased aortic stiffness.[4]

Recently, we have highlighted the association between abnormal aortic arch geometry and late hypertension in patients with anatomically successful CoA repair

Abbreviations and Acronyms

CoA = coarctation of the aorta
FIESTA = fast imaging employing steady-state acquisition
LV = left ventricular
MRI = magnetic resonance imaging
PWV = pulse wave velocity

(no residual obstruction). In two previous studies we have shown that an angulated Gothic arch, so-called because of the typical triangular form of the aortic arch, as seen in Gothic architecture (Figure 1, *A*), is a strong predictor of both resting[5] and exercise-induced[6] hypertension in patients who did not have any significant anatomic stenosis along the aortic arch or at the site of repair.

In this study we have sought to elucidate the mechanisms whereby a Gothic arch might predispose to hypertension using magnetic resonance imaging (MRI) to study central aortic biomechanical properties and systolic wave propagation. We hypothesized that Gothic arch geometry might lead to enhanced systolic wave reflection (generated by the unusual arch angulation) and increased central aortic stiffness, which are both well-known contributors to the development of hypertension.[7-9]

Materials and Methods

Study Subjects

We studied 60 consecutively presenting eligible subjects who attended our institution for routine clinical follow-up after successful CoA repair. All patients had been operated on by means of left posterolateral thoracotomy before 6 months of age. End-to-end anastomosis (n = 32, 53.3%) was performed in case of simple CoA, whereas extended end-to-end anastomosis (n = 28, 46.7%) was performed when CoA was associated with hypoplasia of the aortic arch, as previously described.[10]

Criteria for inclusion were as follows: (1) asymptomatic subjects taking no cardioactive medication; (2) systolic and diastolic blood pressure at rest defined according to the Task Force on High Blood Pressure in Children and Adolescents[11] for children or systolic blood pressure of less than 140 mm Hg and diastolic blood pressure of less than 90 mm Hg for adults; (3) absence of significant associated cardiac anomalies, including bicuspid aortic valve and aortic regurgitation grade of greater than 1/4 on Doppler echocardiography; and (4) absence of clinical and Doppler flow evidence of structural restenosis in the aorta, with a right arm-leg systolic blood pressure gradient at rest of less than 15 mm Hg and a systolic peak flow velocity of less than 3 m/s in the descending aorta with no evidence of diastolic runoff on Doppler echocardiography. Consistent with this, all subjects had an unobstructed aortic arch on MRI (<30% narrowing at the minimum lumen diameter, see below). We excluded patients who had had any previous treatment for recoarctation (balloon angioplasty, stenting, or surgical intervention).

We investigated, using an identical protocol, 20 healthy age-matched volunteers (outpatients found to have innocent murmurs and children of hospital employees). The study was approved by our institutional ethics review committee, and all patients or their guardians provided informed consent.

MRI Acquisition

All studies were performed by using a 1.5-T magnetic resonance system (Signa LX; General Electric Medical Systems, Milwaukee, Wis) with electrocardiographic gating with fiberoptic leads and a thoracic phased-array surface coil for radiofrequency signal detection. After acquisition of axial images of the thorax, long- and short-axis image series of the heart, including the left ventricle, were obtained by using an electrocardiography-gated 2-dimensional fast imaging employing steady-state acquisition (FIESTA) pulse sequence completed during 24 or fewer heartbeats within a single breath hold. To visualize every segment of the thoracic aorta, the entire aorta was imaged in the transverse and oblique sagittal planes by first using cine-segmented FIESTA and next by using conventional gadolinium-enhanced MRI angiography in an oblique sagittal plane. Before gadolinium injection, a gradient echo pulse sequence with velocity encoding was applied in the direction of the section-selection gradient, perpendicular to the aorta, and proximal to the bifurcation of the pulmonary artery, providing area and velocities at, respectively, the central aorta (or ascending aorta) and the descending aorta. The gradient echo pulse sequence was applied with a 7.3- to 7.8-ms repetition time and a 2.7- to 2.9-ms echo time. Maximal velocity encoding was routinely chosen at 150 cm/s and was increased to a maximum of 200 cm/s when aliasing occurred. Other parameters of the magnetic resonance sequence were as follows: flip angle, 40°; view per segment, only 1; cardiac phase, 18 to 30; slice thickness, 8 mm; imaging matrix, 256 × 160 or 256 × 256; and field of view, 20 to 32 cm. The spatial resolution was 1.20 to 1.68 mm in all cases. This pulse sequence generates phase-related pairs of modulus and velocity-encoded images with a temporal resolution of between 15 and 16 ms.

In all subjects systolic and diastolic blood pressures were measured at 2-minute intervals during the MRI scan by using an automated brachial artery sphygmomanometer cuff placed around the right arm (Accutor 4; Datascope Corp, Montvale, NJ). The average blood pressure of the measurement obtained immediately before and immediately after the aortic MRI was used for the physiologic calculations, as described below.

Image Analysis and Calculations

Aortic arch geometry. As previously described,[5,6] we characterized the postcoarctectomy aortic arch shape in 3 categories based on the global geometry of the aortic arch in the left anterior oblique projection: Gothic, crenel, and Romanesque. Briefly, a Gothic arch had a triangular form, a crenel arch had an intermediate rectangular form, and a Romanesque arch had a smooth semicircular form. As previously reported,[5] we also measured the degree of residual stenosis as follows: $100 \times (1 - [Øm/ØD])$, where Øm is the smallest diameter at the anastomosis or other location in the transverse arch and ØD is the diameter of the descending aorta 10 cm distal to the anastomosis. To investigate

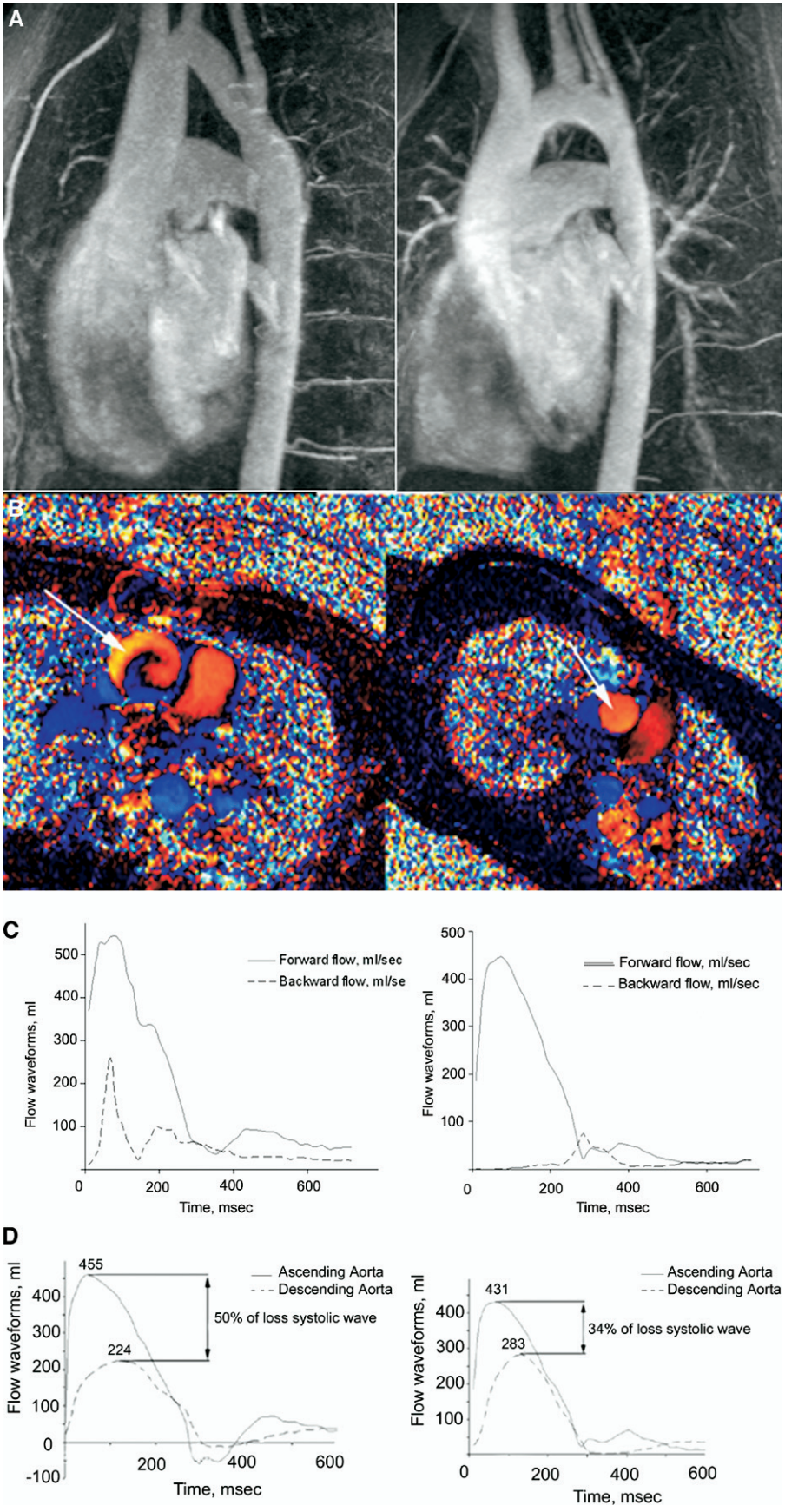

Figure 1. Relation between aortic arch geometry and fluid dynamics. A, Gothic *(left)* and Romanesque *(right)* arch. B, Color technique applied in a section of the ascending aorta, which separates the forward flow *(red)* and backward flow *(blue)* during a cardiac cycle. Please note the skewed systolic backward flow *(white arrow)* in the Gothic aorta, whereas there is no backward flow seen during systole in a Romanesque aorta. C, Flow waveforms during a cardiac cycle illustrating phenomenon described in panel B. There is an early and important systolic backward flow in the Gothic aorta compared with the Romanesque aorta. D, Systolic anterograde wave dissipation across the aortic arch. Please note the important loss of systolic wave amplitude in the Gothic arch compared with the Romanesque arch.

CHD

especially the effect of a Gothic arch and in view of the small numbers of subjects with the crenel (intermediate) form, we excluded the 5 subjects with a crenel arch, and this report focuses on those 55 subjects with Gothic (n = 20) or Romanesque (n = 35) arch anatomy.

Assessment of aortic stiffness. We calculated the following parameters to assess compliance/stiffness of the central and descending aorta in each subject[12,13]:

$$Distensibility = \frac{\Delta A}{A_{diast} \times \Delta P}, \quad (1)$$

$$Compliance = \frac{\Delta A}{\Delta P}, \quad (2)$$

and

$$Aortic\ stiffness\beta\text{-}index = \frac{A_{diast} \times \log \Delta P}{\Delta A}, \quad (3)$$

where ΔA (in millimeters squared) is defined as A_{syst} minus A_{diast}, A_{syst} is the systolic aortic area and A_{diast} is the diastolic aortic area, and ΔP (in millimeters of mercury) is the pulse pressure (ΔP equals systolic blood pressure minus diastolic blood pressure). Excellent interobserver agreement and reproducibility of systolic and diastolic aortic area measurements by using this procedure have been reported previously.[12]

Extraction of flow wave curves. Flow image analysis software (Medis, Leiden, the Netherlands) was used to analyze images. Aortic contours were derived from the modulus images of all cardiac phases. Ascending and descending aorta flow curves were then obtained by using the area of the modulus image and the values of the corresponding encoded velocity image, according to a previously described procedure.[12]

Assessment of aortic pulse wave velocity. Pulse wave velocity (PWV) was calculated by using the transit time (Δt, in seconds) of the systolic flow curves across the aortic arch and the distance (Δd, in meters) between the locations of the measurements at both the ascending and descending aortas (at the level of the pulmonary artery bifurcation): $PWV\,(m/s) = \Delta d/\Delta t$.[11] The distance Δd was calculated from the oblique sagittal image of the central aorta. Transit time (Δt) was generated automatically from the normalized flow curves of the ascending and descending aortas by using an algorithm based on the χ^2 minimization technique written on Matlab version 7.1 software (Mathworks, Sherborn, Mass). In brief, we first extracted the flow waveforms of both the ascending and descending aortas by using the areas on the modulus images and the velocity values of the corresponding velocity-encoded images. Because the flow waveforms were different with regard to their amplitude in the y-axis (the flow waveform was higher in the ascending aorta compared with the descending aorta), they were normalized so that their maximum was equal to 1. Then the interval of time separating the 2 waveforms was determined with a χ^2 minimization technique, which automatically calculated the minimal time (corresponding to the transit time) for which the resemblance between the 2 waveforms was optimal.

Sixteen scans were measured independently by 2 observers blinded to the clinical details of the patients scanned to assess the reliability of these measurements. An excellent interobserver correlation was found in PWVs, with a mean difference of −0.08 ± 0.2 m/s and an interclass correlation coefficient of 0.93.

Assessment of systolic backward flow and energy dissipation across the aortic arch. Forward and backward flows across the sections of the ascending and descending aortas were visualized with a color technique on MRI, which separated the 2 flows in different colors (analogous to that in color Doppler scanning). Forward (or anterograde) flow was visualized in red, and backward (or retrograde) flow was visualized in blue (Figure 1, *B*). Flow waveforms in both the ascending and descending aortas were then extracted, and the volume of backward flow (corresponding to the area under the backward flow curve), as well as the time of the backward flow's appearance in the ascending aorta, was quantified. Backward flow during systole corresponds to systolic wave reflection, and systolic volume is higher in cases in which the systolic wave reflection is enhanced (Figure 1, *C*).

Finally, estimation of the hemodynamic obstruction across the aortic arch was based on the difference in the amplitude of the systolic peak between the ascending and descending waveforms and expressed as the percentage of systolic anterograde wave loss across the arch (Figure 1, *D*).

Assessment of left ventricular mass. Calculation of the left ventricular (LV) mass on MRI was performed by using the standard disc-summation technique.[14] The diastolic and systolic volumes of the left ventricle were measured after determination of epicardial and endocardial borders. LV mass was automatically computed as follows:

$$(Epicardial - Endocardial\ volume) \times Myocardial\ density\ (1.05\ g/mL).$$

Statistical Analysis

All data were stored and analyzed with the R software Version 1.7.0 (R Fondation for Statistical Computing, Vienna, Austria) and the JMP software Version 5.0.1a (SAS Institute, Inc, Cary, NC). Data are presented as the mean value ± standard deviation or median and range where appropriate. Simple linear regression was used to determine the relationships between systolic blood pressure, wave reflection, PWV, and LV mass index. Differences between 2 groups were compared by using the 2-sample (independent) Student *t* test. For assessment of differences between the 3 groups (Gothic, Romanesque, and control), we performed analysis of variance, followed by post-hoc pairwise testing with the Scheffe test.

Results

Clinical Characteristics

Subjects with CoA were aged 16 ± 5 years, and their demographic characteristics are shown in Table 1. The subjects with CoA and control subjects were comparable in age, weight, and height. There was so difference in residual stenosis between the Gothic and Romanaesque groups (Gothic, 14.5% ± 11%; Romanesque, 13.6% ± 9%; $P = .2$). Patients with a Gothic arch were normotensive at rest, but they had a higher resting blood pressure and a

TABLE 1. Baseline characteristics of patients and control subjects

	Gothic (n = 20), mean ± SD (range [median])	Romanesque (n = 35), mean ± SD (range [median])	Control (n = 20), mean ± SD (range [median])	*P* value
Male/female sex	12/8	22/13	13/7	
Age, y	15.3 ± 7 (7.5–32 [12])	15 ± 8 (7–33 [11.5])	14.7 ± 5 (6.5–35 [11.2])	.6
Age at operation, mo	0.3 ± 0.3 (0.1–110 [0.2])	0.3 ± 0.7 (0.15–120 [0.3])		.5
Follow-up after operation, y	15 ± 8 (3–31 [15])	14 ± 7 (4–32 [14.5])		.8
Anthropometry				
Weight, kg	59 ± 18 (28–78 [58])	60 ± 20 (25–80 [60])	59 ± 17 (24–76 [59])	.5
Height, cm	170 ± 17 (135–180 [170])	168 ± 19 (133–178 [169])	171 ± 21 (130–180 [171])	.4
Blood pressure, mm Hg				
Systolic	128 ± 16 (97–137 [128])	118 ± 13 (95–126 [119])	117 ± 10 (87–125 [119])	.04
Diastolic	64 ± 9 (47–75 [65])	67 ± 6 (48–72 [67])	65 ± 5 (50–75 [65])	.1
Pulse pressure	64 ± 7	51 ± 5	52 ± 5	.01

The *P* value for analysis of variance refers to a comparison among the 3 groups. *SD*, Standard deviation.

higher pulse pressure compared with those of patients with a Romanesque arch and control subjects (Table 1).

Aortic Fluid Dynamics

Fluid dynamics were markedly different in the central aorta of patients with a Gothic compared with dynamics of those with a Romanesque arch and compared with control subjects (Table 2). As shown in Figure 1, *B* and *C*, systolic backward flow appeared much earlier in systole in subjects with a Gothic arch (ie, an early return of the incident wave pressure; 22 ± 16 vs 34 ± 10 ms, $P < .0001$). Furthermore, the volume of this systolic backward flow was significantly higher in subjects with a Gothic arch (ie, an enhanced volume, as well as earlier timing of systolic wave reflection) compared with that of subjects with a Romanesque arch (volume 12 ± 6 vs 5 ± 0.3 mL, $P < .0001$). Systolic wave reflection volume correlated significantly with systolic blood pressure ($r^2 = 0.7$, $P < .001$). Consistent with greater wave reflection, there was greater loss of systolic wave amplitude in patients with a Gothic compared with a Romanesque arch (systolic wave amplitude loss of 30% ± 16% vs 22% ± 12%, $P < .01$). There were no differences in systolic backward flow or loss of systolic wave amplitude between patients with a Romanesque arch and control subjects (Table 2).

Aortic Compliance/Stiffness Measurements

Indices of central (precoarctation) aortic distensibility, compliance, and stiffness are shown in Table 2. Biomechanical properties were markedly impaired in patients with a Gothic arch compared with those with a Romanesque arch and control subjects, with decreased distensibility and compliance and increased stiffness β-index ($P < .001$). Patients with a Romanesque arch had increased aortic stiffness compared with that of control subjects. Indeed, they had a higher stiffness β-index (3.9 ± 0.9 vs 2.9 ± 1, $P = .03$), and the PWV had a tendency to be significantly higher (4.1 ± 1 vs 3.5 ± 0.6 m/s, $P = .06$). However, there was no significant difference with regard to compliance and distensibility between patients with a Romanesque arch and control subjects. The PWV across the aortic arch was significantly increased in those with a Gothic arch (5.6 ± 1.1 vs 4.1 ± 1 m/s, $P < .001$), which is consistent with enhanced

TABLE 2. Aortic and ventricular structure and function in the Gothic, Romanesque, and control groups

	Gothic (n = 20)	Romanesque (n = 35)	Control (n = 20)	*P* value
Distensibility, mm $Hg^{-1} \cdot 10^{-3}$	2.9 ± 1	3.8 ± 0.7	4.2 ± 0.5	<.001
Compliance, $mm^2 \cdot mm\ Hg^{-1}$	1.9 ± 0.7	2.6 ± 0.4	2.5 ± 0.6	<.001
Stiffness β-index	5 ± 1.3	3.9 ± 0.9	2.9 ± 1	<.001
PWV, m/s	5.6 ± 1.1	4.1 ± 1	3.5 ± 0.6	<.001
Systolic backward flow volume, mL	12 ± 6	5 ± 0.3	6 ± 1	<.0001
Systolic backward time, ms	22 ± 16	34 ± 10	37 ± 15	<.0001
Loss of systolic wave amplitude across the aortic arch, %	30 ± 16	22 ± 12	15 ± 17	<.01
LV mass index, g/m^2	85 ± 15	77 ± 20	75 ± 18	.04

The *P* value for analysis of variance refers to a comparison among the 3 groups. *PWV*, Pulse wave velocity; *LV*, left ventricular.

rigidity of the central aorta with an angular arch. Furthermore, there was a positive correlation between systolic blood pressure and PWV ($r^2 = 0.7$, $P < .001$).

LV Mass

LV mass index was significantly higher in patients with a Gothic arch compared with the index of those with a Romanesque arch and control subjects (Table 2). There was a positive correlation between systolic blood pressure and LV mass index ($r^2 = 0.7$, $P < .0001$) and between LV mass index and PWV ($r^2 = 0.8$, $P < .0001$). There was no difference in LV mass index between patients with a Romanesque arch and control subjects.

Discussion

The major findings of the present study are that fluid dynamics and aortic biomechanics of the central aorta are markedly abnormal in young normotensive survivors of aortic coarctation repair with an angulated (Gothic) arch compared with those of patients with a smooth rounded (Romanesque) arch. Furthermore, LV mass index was significantly increased in patients with a Gothic arch compared with LV mass index of those with a Romanesque arch, and the LV mass index correlated positively with indices of systolic wave reflection, central aortic stiffness, and systolic blood pressure. Thus our results demonstrate important residual pathophysiologic abnormalities in the central aorta in patients with a Gothic arch, even after "successful" CoA repair, which might be related to the pathogenesis of late hypertension in this clinical setting.

Several previous reports have documented abnormalities of the central aorta, both structural and functional, in patients after anatomically successful CoA repair.[15-19] These abnormalities are likely related to the well-recognized risk of premature cardiovascular morbidity and mortality in young adults after CoA repair.[4] Nevertheless, the factors underlying the appearance of resting or effort-related hypertension in some (approximately 20%-40%) but not all such subjects have not been identified until recently.

With the advent of MRI and its use in all routinely followed survivors of CoA repair at our institution, we recently noted a particular association between an angulated (Gothic-type) arch on MRI and both resting and exercise-induced hypertension.[5,6] We then sought to understand the mechanisms whereby an angulated arch might change fluid dynamics and structure in the central aorta in an attempt to clarify the pathogenesis of hypertension in this setting.

Our hypothesis was that the shaped aortic angle in a Gothic arch would lead to early and large-volume reflection of the systolic wave, which would then lead to higher systolic pressure (by addition of the incident and reflected waves). In addition, enhanced wave reflection would increase wall stress and thus likely induce structural changes in the aortic wall (leading, for example, to increased stiffness and decreased compliance) and also potentially lead to LV hypertrophy (related to both the higher ascending aortic pressure and stiffer aortic mechanical properties).[20-22] These findings were all confirmed in the current study. Interestingly, our study suggests that geometric abnormalities in the aortic arch shape do not entirely explain impairments in aortic elasticity properties. Indeed, patients with a rounded Romanesque arch had increased aortic stiffness compared with that of control subjects. The difference was significant between these two groups with regard to the stiffness β-index. However, we did not find any significant difference when using the other parameters, including PWV, compliance, and distensibility. It might be explained by the small number of subjects in both subgroups (Romanesque, n = 35; control, n = 20).

We were especially careful to exclude subjects with potential confounders of aortic biomechanical properties, such as established hypertension, bicuspid aortic valve, or residual distal stenosis, to allow us to study in isolation the changes caused by a Gothic-type arch versus the more normal-shaped Romanesque-type arch. We speculate that cases of Gothic arch that have already been complicated by hypertension (excluded from the current article) would likely have even greater wave reflection abnormalities, and this requires further study. In patients with a Gothic arch and normotension, it is possible that homeostatic blood pressure-regulating mechanisms (eg, the renin-angiotensin system and central baroreceptors) might be activated to maintain blood pressure within a normal range.

The pathogenesis of Gothic arch is uncertain, although we have recently found that it is not particularly associated with either preoperative aortic arch hypoplasia or with any particular type of surgical repair technique.[6] We hypothesized that a short aortic isthmus might predispose to an angulated arch after repair. Whether identification of the risks associated with a Gothic arch will inform changes in surgical technique will require further experimentation. Nevertheless, the identification of (noninvasively imaged) Gothic arch geometry as a risk factor for aortic stiffness, abnormal wave reflection, and both resting and exercise-induced hypertension serves to identify a high-risk group of young adults. Such subjects require close surveillance and consideration of early medical intervention in view of recent evidence linking aortic stiffness and LV hypertrophy to adverse outcome,[23,24] as well as suggestions that central aortic stiffness might be treatable, with beneficial effects on outcomes (Conduit Artery Function Evaluation study[25]).

In summary, we have found that young adult survivors of aortic CoA repair who have an angulated Gothic aortic arch in follow-up have early and enhanced systolic wave reflection and greater aortic stiffness compared with those characteristics in those whose aortic arch has a more normal

smooth and rounded appearance. These abnormalities of central aortic fluid dynamics and biomechanics predispose to hypertension, LV hypertrophy, and, most likely, adverse cardiovascular outcomes in this group of young adults with repaired congenital heart disease.

References

1. Cohen M, Fuster V, Steele PM, Driscoll D, McGoon DC. Coarctation of the aorta. Long-term follow-up and prediction of outcome after surgical correction. *Circulation*. 1989;80:840-5.
2. O'Sullivan JJ, Derrick G, Darnell R. Prevalence of hypertension in children after early repair of coarctation of the aorta: a cohort study using casual and 24 hour blood pressure measurement. *Heart*. 2002; 88:163-6.
3. Celermajer DS, Greaves K. Survivors of coarctation repair: fixed but not cured. *Heart*. 2002;88:113-4.
4. de Divitiis M, Rubba P, Calabro R. Arterial hypertension and cardiovascular prognosis after successful repair of aortic coarctation: a clinical model for the study of vascular function. *Nutr Metab Cardiovasc Dis*. 2005;15:382-94.
5. Ou P, Bonnet D, Auriacombe L, Pedroni E, Balleux F, Sidi D, et al. Late systemic hypertension and aortic arch geometry after successful repair of coarctation of the aorta. *Eur Heart J*. 2004;25:1853-9.
6. Ou P, Mousseaux E, Celermajer DS, Pedroni E, Vouhe P, Sidi D, et al. Aortic arch deformation following coarctation surgery: effect on blood pressure response. *J Thorac Cardiovasc Surg*. 2006;132:1105-11.
7. London GM. Large artery function and alterations in hypertension. *J Hypertens Suppl*. 1995;13:S35-8.
8. Dernellis J, Panaretou M. Aortic stiffness is an independent predictor of progression to hypertension in nonhypertensive subjects. *Hypertension*. 2005;45:426-31.
9. Willum-Hansen T, Staessen JA, Torp-Pedersen C, Rasmussen S, Thijs L, Ibsen H, et al. Prognostic value of aortic pulse wave velocity as index of arterial stiffness in the general population. *Circulation*. 2006; 113:664-70.
10. Vouhe PR, Trinquet F, Lecompte Y, Vernant F, Roux PM, Touati G, et al. Aortic coarctation with hypoplastic aortic arch. Results of extended end-to-end aortic arch anastomosis. *J Thorac Cardiovasc Surg*. 1988;96:557-63.
11. National High Blood Pressure Education Program Working Group on Hypertension Control in Children and Adolescents. Update on the 1987 task force report on high blood pressure in children and adolescents: a working group report from the National High Blood Pressure Education Program. *Pediatrics*. 1996;98:649-58.
12. Groenink M, de Roos A, Mulder BJ, Verbeeten B Jr, Timmermans J, Zwinderman AH, et al. Biophysical properties of the normal-sized aorta in patients with Marfan syndrome: evaluation with MR flow mapping. *Radiology*. 2001;219:535-40.
13. O'Rourke MF, Staessen JA, Vlachopoulos C, Duprez D, Plante GE. Clinical applications of arterial stiffness; definitions and reference values. *Am J Hypertens*. 2002;15:426-44.
14. Salton CJ, Chuang ML, O'Donnell CJ, Kupka MJ, Larson MG, Kissinger KV, et al. Gender differences and normal left ventricular anatomy in an adult population free of hypertension. A cardiovascular magnetic resonance study of the Framingham Heart Study Offspring cohort. *J Am Coll Cardiol*. 2002;39:1055-60.
15. Sehested J, Baandrup U, Mikkelsen E. Different reactivity and structure of the prestenotic and poststenotic aorta in human coarctation. Implications for baroreceptor function. *Circulation*. 1982;65:1060-5.
16. Xu J, Shiota T, Omoto R, Zhou X, Kyo S, Ishii M, et al. Intravascular ultrasound assessment of regional aortic wall stiffness, distensibility, and compliance in patients with coarctation of the aorta. *Am Heart J*. 1997;134:93-8.
17. Ong CM, Canter CE, Gutierrez FR, Sekarski DR, Goldring DR. Increased stiffness and persistent narrowing of the aorta after successful repair of coarctation of the aorta: relationship to left ventricular mass and blood pressure at rest and with exercise. *Am Heart J*. 1992;123:1594-600.
18. Vogt M, Kuhn A, Baumgartner D, Baumgartner C, Busch R, Kostolny M, et al. Impaired elastic properties of the ascending aorta in newborns before and early after successful coarctation repair: proof of a systemic vascular disease of the prestenotic arteries? *Circulation*. 2005;111: 3269-73.
19. Murakami T, Takeda A. Enhanced aortic pressure wave reflection in patients after repair of aortic coarctation. *Ann Thorac Surg*. 2005;80: 995-9.
20. O'Rourke M. Arterial stiffening and vascular/ventricular interaction. *J Hum Hypertens*. 1994;8(suppl):S9-15.
21. London GM, Guerin A. Influence of arterial pulse and reflective waves on systolic blood pressure and cardiac function. *J Hypertens Suppl*. 1999;17:S3-6.
22. London GM. Role of arterial wall properties in the pathogenesis of systolic hypertension. *Am J Hypertens*. 2005;18(suppl):19S-22S.
23. Roman MJ, Ganau A, Saba PS, Pini R, Pickering TG, Devereux RB. Impact of arterial stiffening on left ventricular structure. *Hypertension*. 2000;36:489-94.
24. Sutton-Tyrrell K, Najjar SS, Boudreau RM, Venkitachalam L, Kupelian V, Simonsick EM, et al. Elevated aortic pulse wave velocity, a marker of arterial stiffness, predicts cardiovascular events in well-functioning older adults. *Circulation*. 2005;111:3384-90.
25. Williams B, Lacy PS, Thom SM, Cruickshank K, Stanton A, Collier D, et al. Differential impact of blood pressure-lowering drugs on central aortic pressure and clinical outcomes: principal results of the Conduit Artery Function Evaluation (CAFE) study. *Circulation*. 2006;113: 1213-25.